J Mol Model (2007) 13: 297–304
DOI 10.1007/s00894-006-0121-3

ORIGINAL PAPER

Heike Meiselbach · Anselm H. C. Horn · Thomas Harrer · Heinrich Sticht

Insights into amprenavir resistance in E35D HIV-1 protease mutation from molecular dynamics and binding free-energy calculations

Received: 25 March 2006 / Accepted: 24 April 2006 / Published online: 23 June 2006

Abstract Drug resistance is a very important factor contributing to the failure of current HIV therapies. The ability to understand the resistance mechanism of HIV-protease mutants may be useful in developing more effective and longer lasting treatment regimens. In this paper, we report the first computational study of the clinically relevant E35D mutation of HIV-1 protease in its unbound conformation and complexed with the clinical inhibitor amprenavir and a sample substrate (Thr-Ile-Met-Met-Gln-Arg). Our data, collected from 10 ns molecular-dynamics simulations, show that the E35D mutation results in an increased flexibility of the flaps, thereby affecting the conformational equilibrium between the closed and semi-open conformations of the free protease. The E35D mutation also causes a significant reduction of the calculated binding free energies both for substrate and amprenavir, thus giving a plausible explanation for its ability to increase the level of resistance. One possible explanation for the emergence of this mutation, despite its unfavorable effect on substrate affinity, might be the role of E35D as an escape mutation, which favors escape from the immune system in addition to conferring drug resistance.

Keywords HIV-1 protease · E35D mutant · Molecular dynamics · MM/PBSA · Drug resistance

Electronic Supplementary Material Supplementary material is available for this article at http://dx.doi.org/10.1001/s00894-006-0121-3 and is accessible for authorized users.

H. Meiselbach · A. H. C. Horn · H. Sticht (✉)
Abteilung für Bioinformatik, Institut für Biochemie,
Emil-Fischer-Zentrum,
Friedrich-Alexander-Universität Erlangen-Nürnberg,
91054 Erlangen, Germany
e-mail: h.sticht@biochem.uni-erlangen.de
Tel.: +49-9131-8524614
Fax: +49-9131-8522485

T. Harrer
Medizinische Klinik III, Klinische Immunologie,
Friedrich-Alexander-Universität Erlangen-Nürnberg,
91054 Erlangen, Germany

Introduction

The Human Immunodeficiency Virus Type-1 (HIV-1), which causes acquired immunodeficiency syndrome (AIDS), is a member of the retrovirus family [1]. HIV-1 protease (PR), part of the aspartic protease family of enzymes, is essential for replication and assembly of the virus. Inactivation of the HIV-1 protease leads to the production of non-infectious viral particles [2]. This viral protein is a homodimer composed of two identical polypeptides of 99 amino acids (Fig. 1a) [3]. The active site is formed at the dimer interface and contains two catalytic aspartic-acid residues.

In recent years, HIV protease has become an important target for the design of antiviral agents for AIDS treatment. However, a major problem shared by current therapies is the rapid development of resistance to antiretroviral drugs by genetic mutation. Mutations can either occur at active-site or non-active-site locations in HIV-1 protease and can also confer different levels of resistance. Primary mutations confer resistance directly to one or more protease inhibitors, whereas secondary mutations only contribute to resistance and often occur together with primary ones or in synergistic form with other secondary mutations. Generally, both types of mutations arise as a consequence of the selective pressure exerted from the medication of protease inhibitors and result in variants of HIV protease that exhibit a decreased binding affinity for inhibitors. One example for the group of secondary non-active-site mutations is E35D, which is observed after treatment of HIV patients with amprenavir (APV) and ritonavir [4].

At least four alternative pathways leading to the development of APV resistance have been identified: the I50V mutation, the V32I mutation plus the I47V mutation, the I54L/M mutation, or, less commonly, the I84V mutation [5, 6]. In addition to these primary mutations, the accumulation of several additional secondary mutations, including E35D, has been shown to increase the level of resistance and to lead to a clear decrease in viral response to treatment [4].

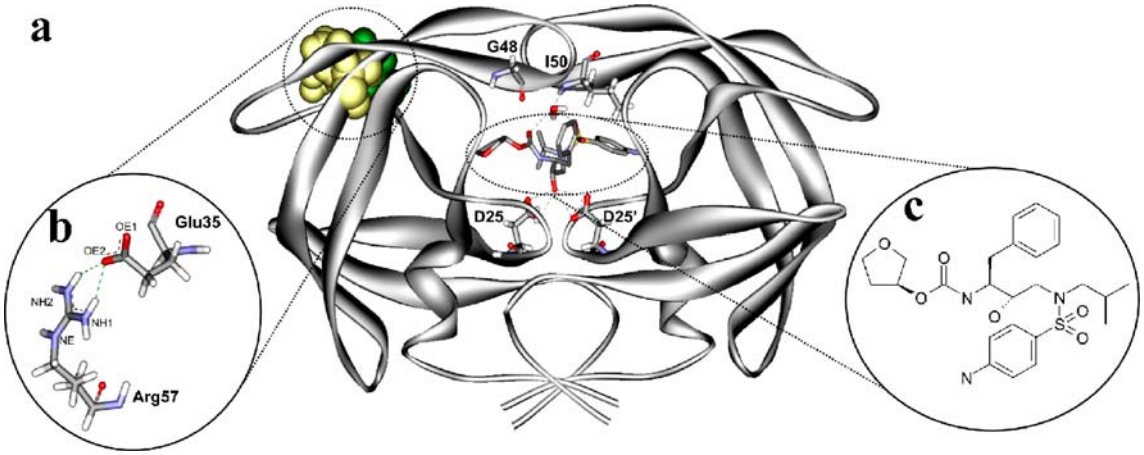

Fig. 1 **a** The structure of the dimeric HIV-1 protease in complex with Amprenavir [10]. The inhibitor, the two catalytic aspatates (D25, D25'), the flap water molecule, and residues G48 and I50 that are important for ligand binding are shown as stick presentation. Residues E35 (*green*) and R57 (*yellow*) are shown in space-filled presentation. **b** *Enlargement* showing the salt bridge between Glu35 and Arg57. **c** *Enlargement* showing the Lewis structure of Amprenavir

To rationalize the effects of the E35D mutation on an atomic level, molecular-dynamics simulations of wild-type and E35D mutant HIV-1 protease were performed for the unbound conformation and complexed with the clinical inhibitor amprenavir and a sample substrate (Thr-Ile-Met-Met-Gln-Arg). In addition, the protease-ligand interaction energies were calculated for wild-type and mutant protease using the MM/PBSA approach. Similar investigations have been carried out previously for several active-site [7–9] and non-active-site [8, 9] mutants and have provided valuable insight into the molecular mechanisms underlying drug resistance.

Materials and methods

Preparation of starting structures

The starting structures of the protease-drug and the protease-substrate complexes were taken from the Protein Data Bank (PDB). The PDB entries were 1HPV for protease complexed with amprenavir [10] (APV) and 4HVP for the protease with bound substrate analogon [11]. The structure of the substrate was generated from the 4HVP crystal structure containing a substrate analog (MVT-101) by replacing the uncleavable CH_2NH linkage between Nle–Nle by a Met–Met peptide bond, leading to a substrate (Acetyl-Thr-Ile-Met-Met-Gln-Arg) as described previously [8, 12]. As no high-resolution crystal structure of an unliganded HIV-1 protease is available, the starting structures of the unbound form were generated by deleting the inhibitor from the APV-bound form following a common approach [7, 13]. The E35D mutant structures were generated using Swiss PDB Viewer [14]. All water molecules present in the crystal structures were maintained throughout the preparation process.

Molecular dynamics simulations

All molecular dynamics (MD) simulations presented in this work were performed using the AMBER 7 program [15, 16] with the parm99 force field [17, 18] and the TIP3P water model [19]. For the organic compound APV, the general AMBER force field (gaff) [20] was used, and missing parameters and partial atomic charges were taken from a previous quantum mechanical parameterization of APV [8].

Simulations were performed in a periodic water box with at least 10 Å of solvent around every atom of the solute. An appropriate number of counterions was added to neutralize the charges of the systems, and the Particle Mesh Ewald summation method [21] was employed to calculate the long-range electrostatic interactions. All structures were minimized in a three-step procedure using the SANDER module of AMBER following a previously established protocol [8].

MD simulations were performed using the SHAKE procedure [22] to constrain all bonds involving hydrogen atoms. The integration time step of the simulation was 1 fs, and an 8.5 Å cutoff was used for the non-bonded interactions, which were updated every 15 steps. The temperature of each system was gradually heated to 298 K during the first 10 ps. Subsequently, 10 ns MD simulations were performed for data collection.

For the visualization and structural analysis of the programs Sybyl 6.9 [23], IsisDraw [24], DS ViewerPro Suite 6 [25], AMBER [16], and X-PLOR [26] were used.

Calculation of binding energies

The binding free energy ΔG_b was calculated according to the standard MM/PBSA approach [27, 28], which is briefly

recapitulated here for the sake of completeness. ΔG_b is calculated according to Eq. 1:

$$\Delta G_b = \Delta G_{MM} + \Delta G_{sol} - T\Delta S, \quad (1)$$

where ΔG_{MM} is the molecular mechanics (MM) interaction energy between protein and ligand, ΔG_{sol} is the solvation free energy, and $-T\Delta S$ is the conformational entropy contribution to the binding. ΔG_{MM} is calculated from the MM interaction energies (Eq. 2):

$$\Delta G_{MM} = \Delta G_{int}^{ele} + \Delta G_{int}^{vdw}, \quad (2)$$

where ΔG_{int}^{ele} and ΔG_{int}^{vdw} are the electrostatic and van der Waals interaction energies between the ligand and the receptor, respectively, which are calculated using the SANDER module in AMBER. Analogously, the solvation free energy, ΔG_{sol}, can be divided into two parts, the electrostatic (ΔG_{sol}^{ele}) and nonpolar ($\Delta G_{sol}^{nonpolar}$) contributions (Eq. 3).

$$\Delta G_{sol} = \Delta G_{sol}^{ele} + \Delta G_{sol}^{nonpolar} \quad (3)$$

The electrostatic contribution to the solvation free energy is calculated via the DelPhi 4 software package [29], which solves the Poisson–Boltzmann equations numerically and calculates the electrostatic energy according to the electrostatic potential. The nonpolar contribution to the solvation free energy is computed as a linear function of the solvent accessible surface area (SA) [30].

$$\Delta G_{sol}^{nonpolar} = \gamma SA + b, \quad (4)$$

with γ=0.00542 kcal mol^{-1} Å^{-2}, and b=0.92 kcal mol^{-1}.

One particular structural feature of HIV-1 protease is the presence of a structural water molecule that bridges the protease flaps with the ligand [10, 11]. Previous studies have demonstrated that explicit consideration of this water molecule is crucial for the calculation of ΔG_b [31]. Thus, this particular water molecule was explicitly included in our MM/PBSA calculation, while the other water molecules were removed before the analysis calculation according to the standard MM/PBSA approach.

Epitope prediction analysis

SYFPEITHI [32], a database of MHC ligands and peptide motifs (http://www.syfpeithi.de/), was used for the epitope prediction. The underlying method relies on the scoring of binding motifs. In particular, the SYFPEITHI matrix applied here is based on the observed amino acid frequencies and the positions of primary anchors to each amino acid at each position in the peptide. The MHC class I molecule (HLA-B*4402) was considered into our analysis.

Results and discussion

Stability of the MD trajectories

Examination of the trajectories obtained from the six MD simulations performed for wild-type and E35D proteases (Fig. 2) shows that all systems deviated to a quite similar extent from their starting structures, resulting in a backbone RMSD of approximately 1.0–1.9 Å after 10 ns. The magnitude of the fluctuations is in the same range as those reported in other recent simulations of HIV-1 protease [7, 8, 31]. One can, therefore, conclude that the simulation runs produced stable trajectories that should provide a suitable basis for the subsequent analyses.

Analysis of the interactions at the site of mutation

In wild-type HIV-1 protease, E35 forms a salt bridge to R57 (Fig. 1b). Although glutamate and aspartate can in principle form the same type of electrostatic side-chain interactions, previous model building based on the static crystal structure of HIV-protease suggested that the shorter side chain of aspartate, compared to glutamate, might result in a larger distance of the charged groups of residues 35 and 57 and, thus, lead to a weaker interaction (data not shown). Therefore, the presence of the salt bridge during the MD simulation was investigated in detail by monitoring the distances between the E/D35 side chain oxygens and the R57 side-chain nitrogens (Fig. 3).

From the panels in Fig. 3, it can be seen that short distances of <3.2 Å between the charged heavy atoms, which are indicative for the presence of a stable salt bridge,

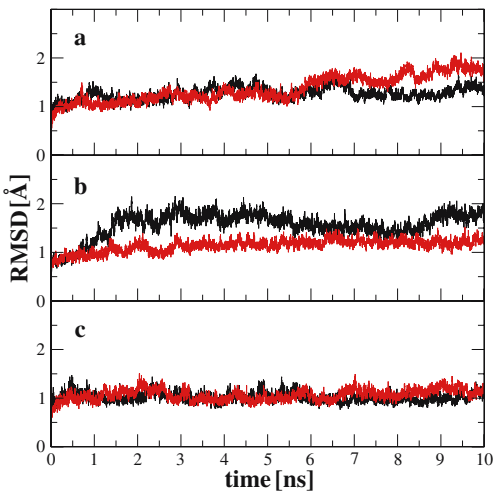

Fig. 2 RMSD of the protease backbone atoms to the starting structure as a function of the simulation time for unliganded (**a**), substrate-bound (**b**), and APV-bound (**c**) protease. *Black*: WT-protease; *red*: E35D mutant

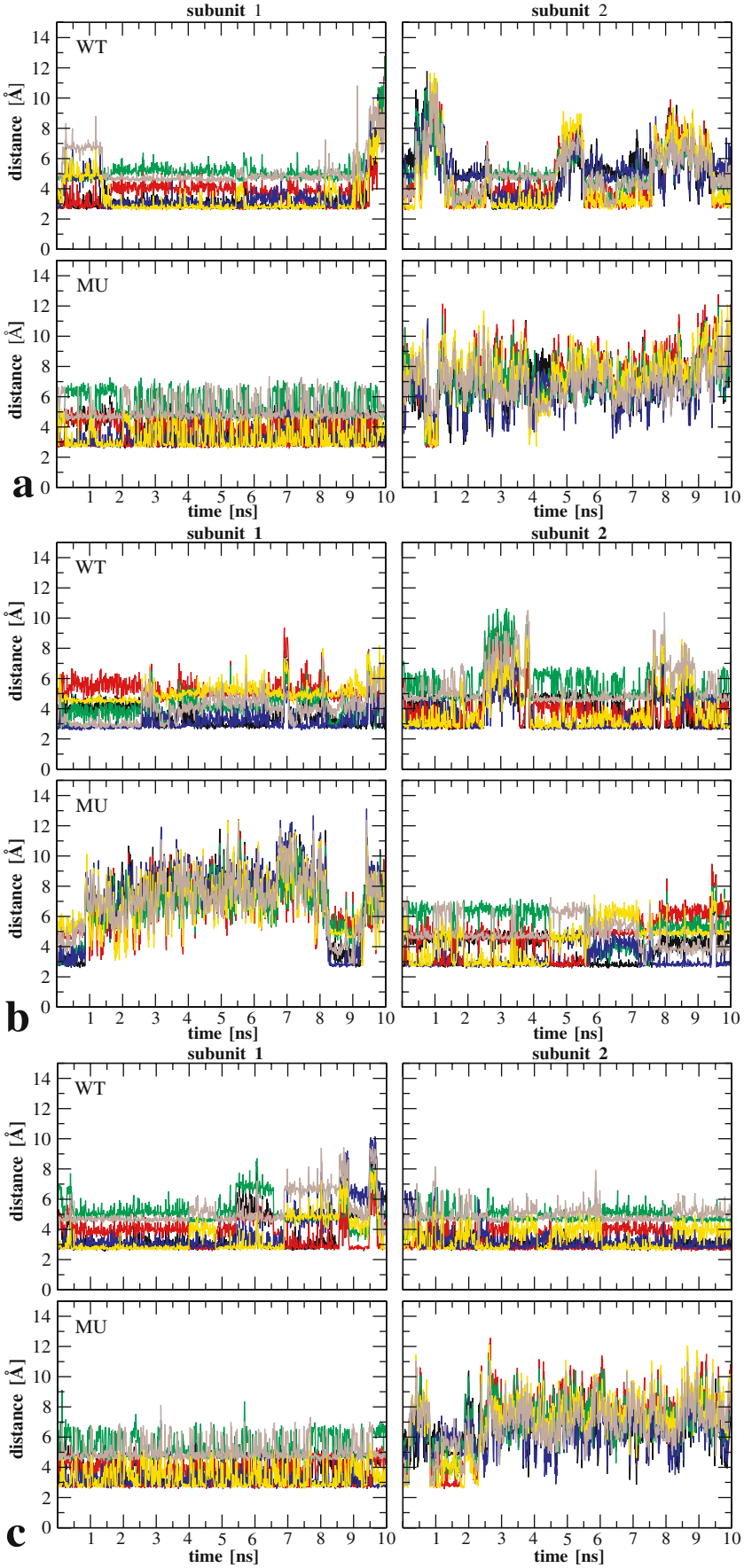
subunit 1
subunit 2
WT
MU
distance [Å]
time [ns]
a
b
c

◀ **Fig. 3** Distances between the side chain oxygens of E/D35 and the side chain nitrogens of R57. Protease: **a** unliganded, **b** complexed with SUB, and **c** complexed with APV. The *upper diagram panels* show the WT and the *lower parts* the mutated systems. The color coding is as follows: $E/D35(O_{\varepsilon 1}/O_{\delta 1}) - R57(N_{\eta 1})$, *black*; $E/D35(O_{\varepsilon 1}/O_{\delta 1}) - R57(N_{\eta 2})$, *red*; $E/D35(O_{\varepsilon 1}/O_{\delta 1}) - R57(N_{\varepsilon})$, *green*; $E/D35(O_{\varepsilon 1}/O_{\delta 2}) - R57(N_{\eta 1})$, *blue*; $E/D35(O_{\varepsilon 1}/O_{\delta 2}) - R57(N_{\eta 2})$, *yellow*; $E/D35(O_{\varepsilon 1}/O_{\delta 2}) - R57(N_{\varepsilon})$, *brown*

are more frequently observed in the simulations of the wild type.

One example, from which this different behavior becomes particularly evident, is subunit 1 of the substrate-bound protease (Fig. 3b). While a stable salt bridge is formed in the wild-type over the entire simulation time, the mutant exhibits stable salt bridges only over short periods of the simulation time (0–1.0 ns, 8.3–9.3 ns). Interestingly, this decreased stability of the salt bridge in the mutant is observed in all simulations, regardless of the type of substrate bound, and also for the unbound protease (Fig. 3; Table 1; Table S1).

The fact that the E35D mutation is located far from the active site and the ligand-binding pocket poses the question by which mechanism this mutation actually confers resistance to the protease. For that purpose, several analyses were performed focusing on structural features like local RMSD values, hydrogen-bonding pattern, and length of the secondary-structure elements. Most of these analyses proved similar properties of wild-type and mutant protease and are, therefore, not discussed in detail in this paper. The most prominent differences between wild-type and mutant protease were observed in the flap region and are, therefore, presented in detail below.

Table 1 Electrostatic interaction energy between the E/D35 and R57 side chain in both subunits of HIV-1 protease

		Energy[a] [kcal mol^{-1}]	
Protease	Ligand	Subunit 1	Subunit 2
WT	Free	−45.45±13.13	−27.44±16.30
E35D	Free	−39.64±7.28	−8.30±7.59
WT	SUB	−35.61±8.64	−38.33±16.03
E35D	SUB	−11.74±12.54	−34.09±7.43
WT	APV	−40.57±13.86	−48.38±7.10
E35D	APV	−40.97±7.37	−9.52±8.75

[a]The electrostatic energy was calculated with the AMBER parm99 force field using a distance-dependent dielectric constant. Water molecules and ions were not included. Mean energy values and standard deviations are based on a total of 10,000 structures collected over the simulation time

Effects of the E35D mutation on the flaps of HIV protease

R57 is located in the antiparallel β-sheet that is part of the protease's flaps (Fig. 1). The flaps represent a functionally important segment that must open to allow substrate access to the active site. Once the appropriate region of the polyprotein is in the active-site, the flaps must close over the substrate to allow cleavage. In the crystal structures of ligand-bound protease, the flaps are in a closed conformation and residues of the flap contribute crucial interactions to substrate or inhibitor binding [10, 11].

In contrast, the flaps of the unliganded protease in solution have been shown by nuclear magnetic resonance (NMR) relaxation studies to be mobile and to move on the 100-μs timescale [33]. Ishima et al. also observed reduced ^{15}N R2 and NOE values for flap residues (Gly49, Ile50, Gly51 and Gly52) that were interpreted as a rapid conformational exchange, on a timescale <<10 ns. This high flexibility can be rationalized by the sequence of the Met-Ile-Gly-Gly-Ile-Gly-Gly-Phe-Ile turn that connects the two strands of the β-sheet.

Recent MD simulations on the nanosecond timescale [7, 34] were able to detect flap-opening motions of HIV protease and pointed out the likely role of these motions in context with the emergence of drug resistance. We have analyzed flap motions in an identical fashion as Perryman et al. [7] by measuring the distances between residue I50 (C_α) located at the tip of the flap and the catalytic residue D25(C_β) (Fig. 4).

Comparison of the distances between the unliganded wild-type and mutant protease clearly shows that the mutant's flaps open farther during the simulation (Fig. 4a). According to a previous definition [7] deduced from a crystal structure of a semi-open form of HIV protease (pdb code: 1HHP) [35], an I50(C_α)–D25(C_β)>15.8 Å corresponds to a semi-open conformation.

While for the wild-type the corresponding distance stays below this threshold over almost the entire simulation time, this threshold is permanently exceeded for both flaps of the mutant during the last third of the simulation time. Thus, a semi-open conformation is observed for the mutant, but not for the wild-type at the end of the simulation time. The final distances reached in the mutant at the end of the simulation are in the range from 18 to 21 Å, which is very similar to the distances observed in a previous 22-ns simulation of the V82F/I84V double mutant that mediates drug resistance [7]. This suggests that the E35D mutation also affects the equilibrium between semi-open and closed conformations, which might represent one mechanism of drug resistance for this mutant.

We also analyzed whether opening of the flaps is also observed in the presence of bound ligands. Analysis of the substrate- and APV-bound proteases (Figs. 4b and c) shows that the I50(C_α)–D25(C_β) distance is <15.8 Å over the entire simulation time, indicating that the protease adopts a closed conformation. This finding is not unexpected, as numerous stabilizing interactions between the flaps of the protease and the bound ligand exist.

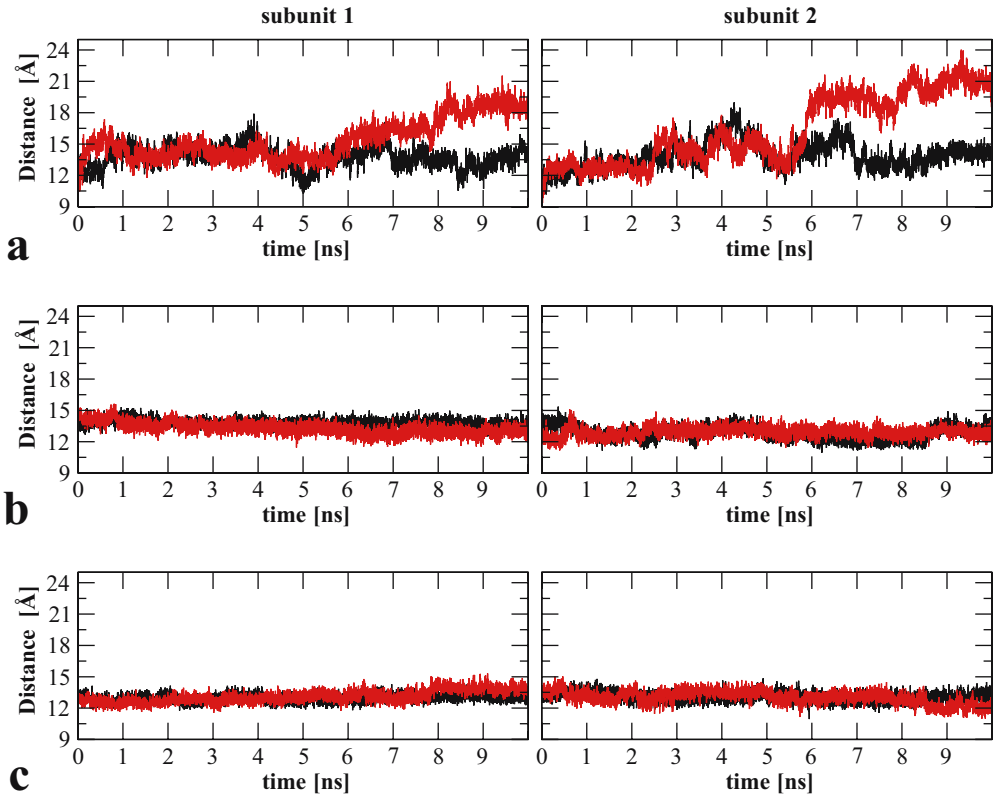

Fig. 4 Comparison of the flap motions by measuring the distance between the tip of the flap I50(C_α) and the catalytic aspartate D25(C_β). Protease: **a** unliganded, **b** complexed with substrate, and **c** complexed with APV. *Black curves* correspond to the wild-type and *red curves* to the mutant system

Subsequently, we analyzed whether these stabilizing interactions are affected by the increased mobility of the flaps that became evident from the simulation of the unbound protease (Fig. 4a). For this purpose, we concentrated on two key interactions that are crucial for substrate and inhibitor binding. The crystal structure of HIV protease in complex with a substrate-based inhibitor (pdb code: 4HVP) [11], which was used as starting structure in our simulation, exhibits a hydrogen bond between the carbonyl oxygen of G48 of the protease's flap and the amide proton of the second residue (I201 in our simulation) of the bound ligand. While this hydrogen bond is stable in the wild-type protease over the entire simulation time (Fig. 5a), larger fluctuations are observed for the mutant protease, suggesting a weaker binding of the substrate.

A similar behavior is observed in the simulation of the APV-bound protease (Fig. 5b). For this complex we have monitored the distance between the amide proton of I50 located in the flap and the sulfonyl-oxygen (O5) of APV. The interaction between the two groups is mediated by a water molecule ('flap-water'; Fig. 1) and has been reported to be crucial for tight APV binding [10]. While the distance between I50(HN) and APV(O5) remains quite constant and similar to that observed in the crystal structure (3.91 Å), a large fluctuation is observed for the mutant at the end of the simulation (Fig. 5b), indicating that this interaction no longer exists.

As evident from Fig. 4c, the loss of this interaction is not accompanied by an opening of the flap. Inspection of the backbone geometry of the flap reveals that the loss of this interaction is rather caused by a local change of the φ-angle of residue I50 from −73° in the starting structure to ~ +60° during the simulation of the APV-bound mutant.

Binding energy calculation

To estimate the effect of the loss of protease–ligand interactions in the E35D mutant on the binding free energy for substrate and APV, an MM/PBSA analysis was performed using 100 snapshots from the last 1 ns of the MD simulation. The calculated binding energies for APV in Table 2 show that the E35D mutation weakens the interaction between protease and inhibitor. The major contribution to this weaker interaction energy comes from the electrostatic energy term, which is consistent with our observation that the motions of the flap affect hydrogen bonds between the protease and the ligand. Interestingly, the E35D mutant also has a significant effect on the substrate binding affinity (Table 2). The decrease of the interaction energy with the substrate is even larger than that observed for APV, suggesting that the E35D mutant has a negative effect on the catalytic activity of the protease.

A quantitative analysis of the effects of the E35D mutation on the binding free energies would require a

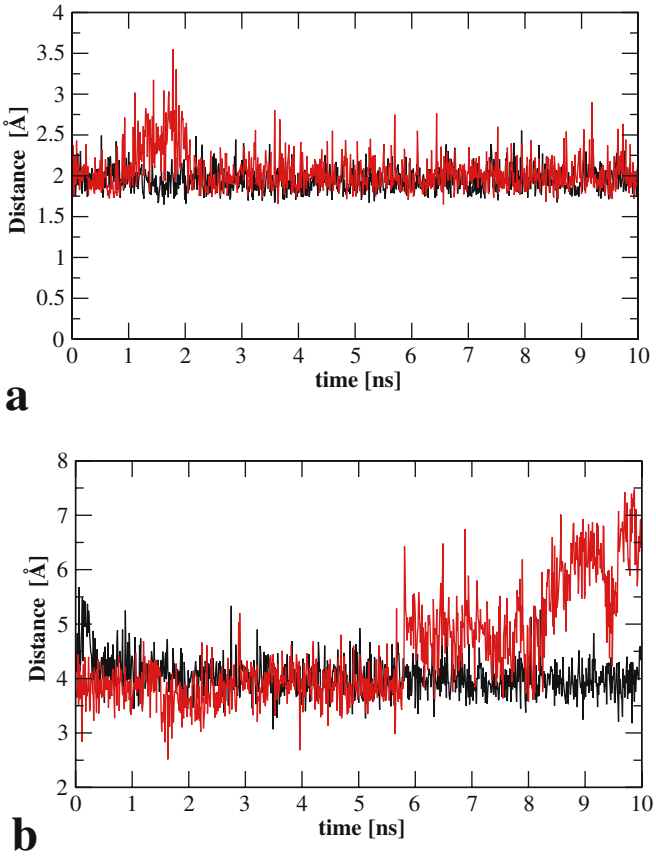

Fig. 5 Distance between **a** residue G48(O) and the substrate residue I201(HN), and **b** residue I50 (HN) to APV(O5) as a function of the simulation time. *Black curves* correspond to the wild-type and *red curves* to the mutant system

consideration of entropic effects. As quantitative measures of entropic contributions are inherently difficult to obtain, we only performed a qualitative estimate of the conformational entropy contributions of the wild-type and mutant protease on the binding free energy: The conformational entropy of the ligand-bound wild-type and mutant protease appear to be similar, as none of them are observed to undergo larger conformational changes over the entire simulation time. In contrast, a semi-open flap conformation is observed for the unliganded mutant, but not for the unbound wildtype protease. Therefore, the loss of conformational entropy upon ligand binding is expected to be larger in the mutant protease than in the wild-type protease. As this effect is not taken into account in Table 2, the calculated differences of the binding free energies (15.58 and 6.89 kcal mol^{-1} for SUB and APV, respectively) are expected to underestimate the magnitude of the affinity decrease caused by the E35D mutant.

Putative selective mechanisms promoting the emergence of the E35D mutation

The large effect of the E35D mutation on the affinity for the substrate poses the question whether the selective pressure arising from APV treatment alone is sufficient for the emergence of the E35D mutation and suggests that additional selection mechanisms might be involved.

Recent studies have shown that, besides the selective pressure exerted by antiviral agents, immunological pressure represents a second cause for the emergence of mutations in HIV protease [36–38]. The latter pressure is exerted by the immune system, in which human leucocyte antigens (HLA) bind peptide epitopes originating from the HIV protease and presents them on the cell surface, thus triggering the cellular immune response. "Escape mutations" in the corresponding epitopes or the HIV protease impede this recognition process and lead to a suppression of the cellular immune response.

A role as escape mutation is quite plausible for E35D, because it is located in an epitope (E**E**MSLPGRW) that is recognized by HLA allele B44 [39]. In addition, E35 is the N-terminal anchoring residue of this epitope, underlining its importance for HLA binding [39, 40]. To substantiate this hypothesis, we have calculated the probability that the wild-type and mutant sequences (EEMSLPGRW and EDMSLPGRW) represent HLA-B44 epitopes. The score, which indicates the likelihood of an interaction with HLA-B44, is significantly decreased by a factor of two, indicating that this mutant very likely facilitates escape of the virus from the immune system. Thus, this mutation is expected to arise preferentially when both selective pressure and immunological pressure exist in an infected host.

Conclusions

In summary, our data show that the E35D mutation causes an increased flexibility of the flaps, thereby affecting the

Table 2 Binding free energies (in kcal mol^{-1}) of the HIV-1 protease (WT and E35D) associated with substrate (SUB) and amprenavir (APV), calculated using the MM/PBSA strategy as described in the Materials and methods section

	ΔG_{int}^{vdw}	ΔG_{int}^{ele}	$\Delta G_{sol}^{nonpolar}$	ΔG_{sol}^{ele}	ΔG_{b}^{a}
WT-protease-SUB	−78.42	−91.51	−6.25	123.45	−52.73
E35D-protease-SUB	−84.12	−73.81	−6.89	127.67	−37.15
WT-protease -APV	−58.81	−50.82	−5.00	37.69	−76.94
E35D-protease-APV	−56.30	−49.36	−4.89	40.50	−70.05

[a] $\Delta G_b = \Delta G_{int}^{vdw} + \Delta G_{int}^{ele} + \Delta G_{sol}^{nonpolar} + \Delta G_{sol}^{ele}$
The entropic contribution, $-T\Delta S$, is not included (see text for details)

conformational equilibrium between the closed and semi-open conformations of the free protease. In addition, the mutation results in a decreased affinity for both the substrate and the inhibitor APV, thus giving a plausible explanation for its ability to increase the level of resistance. One possible explanation for the emergence of this mutation despite its unfavorable effect on substrate affinity might be that E35D plays a role as an escape mutation that favors escape from the immune system in addition to conferring drug resistance.

Acknowledgements This work was supported by grants from the Deutsche Forschungsgemeinschaft (SFB466, B6, and C11) to T. H. and H. S. and by the Competence Network HIV/AIDS (Project F2) to T. H. The authors thank the Regionales Rechenzentrum Erlangen (RRZE) for technical support.

References

1. Mitsuya H, Yarchoan R, Broder S (1990) Science 249:1533–1544
2. Kohl NE, Emmi EA, Schleif WA, Davies LJ, Heimbach JC, Dixon RAF (1988) Proc Natl Acad Sci 85:686–690
3. Meek TD, Dayton BD, Metcalf BW, Dreyer GB, Strickler JE, Gorniak JG, Rosenberg M, Moore ML, Magaard VW, Debouck C (1989) Proc Natl Acad Sci USA 86:1841–1845
4. Arvieux C, Tribut O (2005) Drugs 65:633–659
5. Marcelin AG, Lamotte C, Delaugerre C, Ktorza N, Ait Mohand H, Cacace R, Bonmarchand M, Wirden M, Simon A, Bossi P, Bricaire F, Costagliola D, Katlama C, Peytavin G, Calvez V (2003) Antimicrob Agents Chemother 47:594–600
6. Tisdale M, Myers R, Randall S, Maguire M, Ait-Khaled M, Elston R, Snowden W (2000) Clin Drug Investig 20:267–285
7. Perryman AL, Lin JH, McCammon JA (2004) Protein Sci 13:1108–1123
8. Wartha F, Horn AHC, Meiselbach H, Sticht H (2005) J Chem Theory Comput 1:315-324
9. Ode H, Ota M, Neya S, Hata M, Sugiura W, Hoshino T (2005) J Phys Chem B 109:565–574
10. Kim EE, Baker CT, Dwyer MD, Murcko MA, Rao BG, Tung RD, Navia MA (1995) J Am Chem Soc 117:1181–1182
11. Miller M, Schneider J, Sathyanarayana BK, Toth MV, Marshall GR, Clawson L, Selk L, Kent SB, Wlodawer A (1989) Science 246:1149–1152
12. Piana S, Carloni P, Röthlisberger U (2002) Protein Sci 11:2393–2402
13. Kaldor SW, Kalish VJ, Davies JF, 2nd, Shetty BV, Fritz JE, Appelt K, Burgess JA, Campanale KM, Chirgadze NY, Clawson DK, Dressman BA, Hatch SD, Khalil DA, Kosa MB, Lubbehusen PP, Muesing MA, Patick AK, Reich SH, Su KS, Tatlock JH (1997) J Med Chem 40:3979–3985
14. Guex N, Peitsch MC (1997) Electrophoresis 18:2714–2723
15. Case DA, Pearlman DA, Caldwell JW, Cheatham TE III, Wang J, Ross WS, Simmerling CL, Darden TA, Merz KM, Stanton RV, Cheng AL, Vincent JJ, Crowley M, Tsui V, Gohlke H, Radmer RJ, Duan Y, Pitera J, Massova I, Seibel GL, Singh UC, Weiner PK, Kollman PA (2002) Amber 7. University of California, San Francisco, USA
16. Pearlman DA, Case DA, Caldwell JW, Ross WS, Cheatham TE III, de Bolt S, Ferguson D, Seibel G, Kollman P (1995) Comput Phys Commun 91:1–41
17. Cheatham TE III, Cieplak P, Kollman PA (1999) J Biomol Struct Dyn 16:845-862
18. Cornell WD, Cieplak P, Bayly CI, Gould IR, Merz KMJ, Ferguson DM, Spellmeyer DC, Fox T, Caldwell JW, Kollman PA (1995) J Am Chem Soc 117:5179–5197
19. Jorgensen WL, Chandrasekhar J, Madura JD, Impey RW, Klein ML (1983) J Chem Phys 79:926–935
20. Wang J, Wolf RM, Caldwell JW, Kollman PA, Case DA (2004) J Comput Chem 25:1157–1174
21. Darden TA, York DM, Pedersen LG (1993) J Chem Phys 98:10089–10092
22. Ryckaert JP, Ciccotti G, Berendsen HJC (1977) J Comput Phys 23:327–341
23. Tripos (1991–2002) Sybyl 6.9, Release 7.0A. St. Louis, Missouri, USA
24. MDL (1990-2000) ISIS/Draw 2.3. San Leandro, CA, USA
25. Accelrys (2005) DS ViewerPro Suite 6.0. San Diego CA
26. Brünger AT (1992) Yale University Press, New Haven, CT
27. Kollman PA, Massova I, Reyes C, Kuhn B, Huo S, Chong L, Lee M, Lee T, Duan Y, Wang W, Donini O, Cieplak P, Srinivasan J, Case DA, Cheatham TE III (2000) Acc Chem Res 33:889–897
28. Srinivasan J, Cheatham TE III, Cieplak P, Kollman PA, Case DA (1998) J Am Chem Soc 120:9401–9409
29. Gilson MK, Sharp KA, Honig B (1987) J Comput Chem 9:327-335
30. Sitkoff D, Sharp KA, Honig B (1994) J Phys Chem 1978–1988
31. Lepsik M, Kriz Z, Havlas Z (2004) Proteins 57:279–293
32. Rammensee H, Bachmann J, Emmerich NP, Bachor OA, Stevanovic S (1999) Immunogenetics 50:213–219
33. Ishima R, Freedberg DI, Wang YX, Louis JM, Torchia DA (1999) Structure (Lond) 7:1047–1055
34. Scott WR, Schiffer CA (2000) Structure (Lond) 8:1259–1265
35. Spinelli S, Liu QZ, Alzari PM, Hirel PH, Poljak RJ (1991) Biochimie 73:1391–1396
36. Leslie A, Kavanagh D, Honeyborne I, Pfafferott K, Edwards C, Pillay T, Hilton L, Thobakgale C, Ramduth D, Draenert R, Le Gall S, Luzzi G, Edwards A, Brander C, Sewell AK, Moore S, Mullins J, Moore C, Mallal S, Bhardwaj N, Yusim K, Phillips R, Klenerman P, Korber B, Kiepiela P, Walker B, Goulder P (2005) J Exp Med 201:891–902
37. Leslie AJ, Pfafferott KJ, Chetty P, Draenert R, Addo MM, Feeney M, Tang Y, Holmes EC, Allen T, Prado JG, Altfeld M, Brander C, Dixon C, Ramduth D, Jeena P, Thomas SA, St John A, Roach TA, Kupfer B, Luzzi G, Edwards A, Taylor G, Lyall H, Tudor-Williams G, Novelli V, Martinez-Picado J, Kiepiela P, Walker BD, Goulder PJ (2004) Nat Med 10:282–289
38. Moore CB, John M, James IR, Christiansen FT, Witt CS, Mallal SA (2002) Science 296:1439–1443
39. Sidney J, Southwood S, Pasquetto V, Sette A (2003) J Immunol 171:5964–5974
40. Rodriguez WR, Addo MM, Rathod A, Fitzpatrick CA, Yu XG, Perkins B, Rosenberg ES, Altfeld M, Walker BD (2004) J Transl Med 2:15